

JAERI - M  
88-174

ANALYSIS OF INVERTED ANNULAR FILM BOILING  
BY THE MINCS CODE USING TWO-FLUID MODEL

September 1988

Kaiming WANG\*, Tadashi WATANABE and Masashi HIRANO

JAERI-Mレポートは、日本原子力研究所が不定期に公開している研究報告書です。  
入手の間合わせは、日本原子力研究所技術情報部情報資料課（〒319-11茨城県那珂郡東  
海村）あて、お申しこしてください。なお、このほかに財団法人原子力弘済会資料センター  
（〒319-11茨城県那珂郡東海村日本原子力研究所内）で複写による実費頒布をおこなって  
おります。

**JAERI-M reports are issued irregularly.**

**Inquiries about availability of the reports should be addressed to Information Division  
Department of Technical Information, Japan Atomic Energy Research Institute, Tokai-  
mura, Naka-gun, Ibaraki-ken 319-11, Japan.**

©Japan Atomic Energy Research Institute, 1988

編集兼発行 日本原子力研究所  
印刷 關高野高速印刷

Analysis of Inverted Annular Film Boiling  
by The MINCS Code Using Two-Fluid Model

Kaiming WANG \*

Tadashi WATANABE and Masashi HIRANO

Department of Nuclear Safety  
Tokai Research Establishment  
Japan Atomic Energy Research Institute  
Tokai-mura, Naka-gun, Ibaraki-ken

(Received August 22, 1988)

A set of new constitutive relations appropriate to Inverted Annular Film Boiling regime has been developed based on Aritomi's experiment using Freon-113. Conservation equations for two-fluid model together with proposed constitutive relations were solved numerically by the two-phase flow analyzer MINCS which had been developed at Japan Atomic Energy Research Institute. Calculated results for the Aritomi's test were in good agreement with the experimental results. The proposed model were applied to the analysis of Stewart's experiment using water for verification. A better agreement between calculated and experimental results was also obtained at relatively low pressure condition. The effects of liquid inlet subcooling, pressure and flow rate on wall heat transfer coefficient were discussed.

Keywords: Safety Analysis, LOCA, Reflood, Two-fluid Model, Two-phase flow, Inverted Annular Film Boiling, Constitutive Relations

---

\* on leave from Southwest Nuclear Reactor Engineering Research and Design Institute, China

MINCSコードによる二流体モデルを用いた逆還状二相流膜沸騰現象の解析

日本原子力研究所東海研究所原子炉安全工学部

王 开明\*・渡辺 正・平野 雅司

(1988年8月22日受理)

逆環状二相流膜沸騰領域に対する構成式を、フロン-113を用いた有富の実験に基づいて新たに作成した。二流体モデルの保存方程式が、提唱された構成式と共に数値的に解かれた。解析には、日本原子力研究所に於いて開発された過渡二相流解析コードMINCSを使用した。有富の実験に対する計算結果は、実験結果と良く一致した。さらに、提唱された構成式の適用性を調べる為にStewartの実験解析をおこなった。比較的低圧の状態に於いて、計算結果と実験結果の良好な一致を得た。流入する液体のサブクール度、圧力、流量の壁面熱伝達係数に及ぼす影響について考察を行った。

## Contents

1. Introduction .....	1
2. Two-fluid model .....	4
2.1 Two-fluid conservation equations .....	4
2.2 Constitutive relations .....	5
3. Calculated results and discussion .....	11
3.1 Comparison with Aritomi's experiment .....	11
3.2 Comparison with Stewart's experiment .....	12
4. Summary and conclusion .....	25
Acknowledgement .....	26
References .....	27
Appendix A Input Model of MINCS for IAFB .....	30
Appendix B Physical Properties of Freon-113 .....	43

## 目 次

1. 序 .....	1
2. 二流体モデル .....	4
2.1 二流体モデルの保存式 .....	4
2.2 構成式 .....	5
3. 計算結果及び議論 .....	11
3.1 Aritomiの実験との比較 .....	11
3.2 Stewartの実験との比較 .....	12
4. まとめ及び結論 .....	25
謝 辞 .....	26
参考文献 .....	27
付録 A 逆環状膜沸騰流のMINCSへの入力モデル .....	30
付録 B フレオン-113の物性 .....	43

## Nomenclature

A	cross-sectional flow area
B	ratio of temperature difference
C <sub>p</sub>	specific heat
D	diameter
D <sub>e</sub>	hydraulic equivalent diameter
D <sub>h</sub>	thermodynamic equivalent diameter
f	friction factor
F	wavy interface influence factor
g	gravitational constant
h	enthalpy
H	heat transfer coefficient
k	thermal conductivity
Nu	Nusselt number
p	pressure
P	perimeter
Pr	Prandtl number
q	heat flux
r	radius
Re	Reynolds number
t	time
T	temperature
U	velocity
z	axial coordinate

## Greek letters

$\alpha$	volume fraction
$\delta$	vapour film thickness
$\Gamma$	mass transfer rate
$\epsilon$	emissivity
$\theta$	influence coefficient
$\mu$	viscosity
$\pi$	rate of circumference

$\rho$	density
$\sigma_B$	Stefan-Boltzman constant
$\sigma$	surface tension
$\tau$	shear stress

Subscripts

i	interface
l	liquid phase
rad	radiation
s	saturation
sub	subcooled
v	vapour phase
w	wall

## 1. Introduction

In recent years, a number of advanced, best-estimate system codes such as TRAC <sup>(1,2)</sup> and RELAP5 <sup>(3)</sup> have been developed to predict the consequences of various postulated accidents and transients in light water reactors (LWRs). Although these codes have gone through assessment to some extent during the developmental stage, it is recognized that the evaluation of constitutive relations using experimental data is still of importance. From this point of view, the transient two-phase flow analyzer: the MINCS code <sup>(4,5)</sup> has been developed at Japan Atomic Energy Research Institute (JAERI) as a computational tool for the development and assessment of various constitutive relations mainly through analysis of separate effect tests. The main purpose of this study is to develop the inverted annular film boiling (IAFB) model for two-fluid model using MINCS.

The inverted annular film boiling appears when stable vapour film covers heated wall and the liquid phase is continuous in core as shown in Fig. 1.1 Under certain accident conditions in LWRs, for example, during the reflooding stage of a large break loss-of-coolant accident (LOCA), IAFB may occur in the reactor core where the fuel clad temperature exceeds the minimum film boiling temperature and the coolant is subcooled. Accurate knowledge of IAFB is required in order to predict overall system safety: effectiveness of the emergency core cooling system, fuel clad temperature and so on. The IAFB phenomena appear not only in the LWRs' accident but in other engineering fields such as cryogenics in which low quality boiling occurs.

In the ideal IAFB regime, flows of liquid and vapour phases are separated and the liquid phase can not contact with the heating wall. The non-equilibrium thermal-hydraulic phenomena appear in this regime. The vapour film is superheated, but the continuous liquid core is subcooled. Heat is transferred from the wall to the vapour and from the vapour to the liquid. For a subcooled liquid core, a part of heat from vapour is used for vaporization and another part for reducing the subcooling. Vaporization of liquid occurs at the interface of vapor and liquid. The direct vapour-wall contact reduces the heat transfer rate and results in high wall temperature.



The two-phase flow and heat transfer phenomena in IAFB are very complex. The interface of liquid and vapour possibly becomes wavy because of vaporization and large velocity difference between liquid and vapour. This phenomenon has been observed by Ishii <sup>(6)</sup>. The random disturbance at the liquid-vapour interface in a pool film boiling has been studied by Coury et. al. <sup>(7,8)</sup>. This disturbance may result in intermittent touching of the liquid with the wall <sup>(9,10)</sup>. The subcooled liquid core may contain bubbles and vapour film may contain liquid droplets <sup>(10)</sup>. Presently, the consideration of such detailed effects in an analytical model is very difficult.

Although the development of research for IAFB is rapid and many models based on experiments have been proposed, they have always some limits which result in difficulty to extend their applied ranges. The early analysis by Dougall and Rohsenow <sup>(11)</sup> has accounted for the turbulence in the vapour film, but was applied only to saturated liquid. Elias and Chambre <sup>(12)</sup> have solved the entrance-region problem for the vapour film. However, their model was based on a number of rather drastic assumptions, for example, the vapour was generated at the quench front only, with the wall and liquid at constant temperatures. Osakabe and Sudo <sup>(13)</sup> have proposed a solution accounting for the turbulence in the vapour film and correcting the effect of void fraction in the mixture core. However, their model considered only saturated flow and ignored the velocity of the liquid phase.

The development of the two-fluid model <sup>(14,15)</sup> makes detailed analysis of IAFB possible. The understanding of interaction between two phases becomes indispensable when the two-fluid model is used. Most of experimental research was performed to observe heat transfer phenomena between the heated wall and the fluid <sup>(16,17,18,19)</sup>. Although a large number of heat transfer correlations were proposed as reviewed by Croeneveld <sup>(20,21)</sup>, there is little understanding of the basic hydrodynamics. The main reason for the lack of information about the flow characteristics is due to experimental difficulties associated with flow measurement. From above view, it is recognized that the understanding of mechanisms and the establishment of an analytical model for IAFB are necessary.

The thermal and hydraulic behavior of inverted annular flow have been investigated experimentally under various conditions of heat flux,

inlet velocity, inlet subcooling and heating length using Freon-113 by Aritomi<sup>(22)</sup>. It was shown that the experimental results of vapour film thickness and heat transfer coefficient were not in good agreement with those by Bromley's<sup>(23)</sup> or Sudo's<sup>(13)</sup> correlations. The empirical correlations were proposed for the net vaporization rate from the interface, interfacial shear stress and heat transfer coefficients from wall to vapour and from interface to liquid.

In this study, the constitutive relations for IAFB in two-fluid model are proposed based on Aritomi's empirical correlations. Conservation equations for two phases are solved together with the proposed constitutive relations by using MINCS. The comparison of calculated results with experimental data for Aritomi's test is performed. Then, the proposed model is applied to the analysis of Stewart's experiment for verification. The effects of liquid inlet subcooling, pressure and flow rate on wall heat transfer coefficient are discussed.

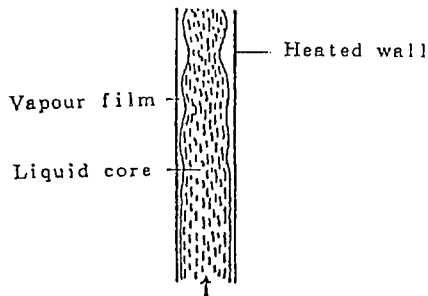


Fig. 1.1 Sketch of IAFB

## 2. Two-fluid model

In this section, the thermo-hydraulic conservation equations for two-fluid model are described and constitutive relations for IAFB regime are proposed.

### 2.1 Two-fluid conservation equations

The two-fluid formulation uses a separate set of conservation equations (mass, momentum and energy) for each phase. The flow regime of IAFB is assumed as an ideal regime in which there are not any entrainments in both phases and the liquid core is not in touch with the wall.

#### 2.1.1 Mass conservation equations

$$A \frac{\partial (\alpha_l \rho_l)}{\partial t} + \frac{\partial (\alpha_l \rho_l U_l A)}{\partial z} - P_i \Gamma_{li} \quad (1)$$

$$A \frac{\partial (\alpha_v \rho_v)}{\partial t} + \frac{\partial (\alpha_v \rho_v U_v A)}{\partial z} - P_i \Gamma_{vi} \quad (2)$$

#### 2.1.2 Momentum conservation equations

$$A \alpha_l \rho_l \frac{\partial U_l}{\partial t} + A \alpha_l \rho_l U_l \frac{\partial U_l}{\partial z} + A \alpha_l \frac{\partial P_l}{\partial z} - P_i \Gamma_{li} (U_i - U_l) + P_i \tau_{li} - P_i \tau_{lw} + A \alpha_l \rho_l g_z \quad (3)$$

$$A \alpha_v \rho_v \frac{\partial U_v}{\partial t} + A \alpha_v \rho_v U_v \frac{\partial U_v}{\partial z} + A \alpha_v \frac{\partial P_v}{\partial z} - P_i \Gamma_{vi} (U_i - U_v) + P_i \tau_{vi} - P_i \tau_{vw} + A \alpha_v \rho_v g_z \quad (4)$$

#### 2.1.3 Energy conservation equations

$$\begin{aligned} A \frac{\partial \{ \alpha_l \rho_l (h_l + \frac{U_l^2}{2}) \}}{\partial t} + \frac{\partial \{ A \alpha_l \rho_l U_l (h_l + \frac{U_l^2}{2}) \}}{\partial z} - \alpha_l \frac{\partial P_l}{\partial t} \\ - P_i \Gamma_{li} (h_{li} + \frac{U_{li}^2}{2}) + P_i q_{li} + P_{lw} q_{lw} + A \alpha_l \rho_l U_l g_z \end{aligned} \quad (5)$$

$$\begin{aligned}
 A \frac{\partial (\alpha_v \rho_v (h_v + \frac{U_v^2}{2}))}{\partial t} + \frac{\partial (A \alpha_v \rho_v U_v (h_v + \frac{U_v^2}{2}))}{\partial z} - \alpha_v \frac{\partial p_v}{\partial t} \\
 - P_i \Gamma_{vi} (h_{vi} + \frac{U_{vi}^2}{2}) + P_i q_{vi} + P_{vw} q_{vw} + A \alpha_v \rho_v U_v g_x
 \end{aligned} \quad (6)$$

In Eqs.(1) to (6), subscripts  $l$ ,  $v$ ,  $i$  and  $w$  denote liquid phase, vapour phase, interface of two phases and wall, respectively, and volume fractions of liquid and vapour ( $\alpha_l, \alpha_v$ ) satisfy

$$\alpha_l + \alpha_v = 1 . \quad (7)$$

We, approximately, assume that

$$p_l = p_v = p \quad \text{and} \quad (8)$$

$$U_i = \min(U_l, U_v) . \quad (9)$$

Basic state variables  $\alpha_k$ ,  $p$ ,  $h_k$  and  $U_k$  ( $k=l, v$ ) can be obtained by solving equations (1) to (6), and other variables  $A$ ,  $P_i$ ,  $P_{kw}$ ,  $\rho_k$ ,  $q_k$ ,  $\tau_{kj}$  and  $\Gamma_{ki}$  ( $j=i, w$  and  $k=l, v$ ) are determined by constitutive relations.

## 2.2 Constitutive relations

To close the system, constitutive relations are needed for  $P_i$ ,  $P_{kw}$ ,  $\rho_k$ ,  $q_k$ ,  $\tau_{kj}$  and  $\Gamma_{ki}$  as a function of basic state variables,  $\alpha_k$ ,  $p$ ,  $h_k$  and  $U_k$ . In the following, the constitutive relations are described in detail.

### 2.2.1 Geometrical conditions

The cross-sectional area  $A$  of a cylindrical test tube of diameter  $D$  is

$$A = \frac{\pi}{4} D^2 . \quad (10)$$

For IAFB regime, it is assumed that the vapour flows in a vertical annular channel which is constructed by the tube wall and the liquid-vapour interface, and the liquid phase flows in a circular tube

which is bounded by the interface. The vapour film thickness  $\delta$  and interfacial perimeter  $P_i$  are related to the vapour fraction  $\alpha_v$  by

$$\delta = \frac{D}{2}(1 - \sqrt{1 - \alpha_v}), \quad (11)$$

$$P_i = \pi(D - 2\delta). \quad (12)$$

The perimeters of vapour-wall and liquid-wall are

$$P_{vw} = \pi D \quad \text{and} \quad P_{lw} = 0. \quad (13)$$

### 2.2.2 The equations of state

The thermodynamic equations of state are given by

$$\rho_k = \rho_k(p, h_k) \quad \text{and} \quad T_k = T_k(p, h_k), \quad (14)$$

where  $T_k$  is the k-phase temperature. These relations are supplied by MINCS so long as water is used.

### 2.2.3 Wall shear stresses

Because the wall is covered by vapour film only, the wall shear stresses are assumed as follows:

$$r_{lw} = 0 \quad \text{and} \quad (15)$$

$$r_{vw} = \frac{1}{2} f_{vw} \rho_v |U_v| U_v, \quad (16)$$

where  $f_{vw}$  denotes the friction factor of vapour-wall. We use the Colebrook's correlation <sup>[24]</sup> for  $f_{vw}$ . The wall friction  $f_{vw}$  is given by

$$(1) \quad Re_v < 1000$$

$$f_{vw} = \frac{16.0}{Re_v},$$

$$(2) \quad Re_v > 4000$$

$$\frac{1}{\sqrt{4f_{vw}}} = 0.86 \log \left( \frac{2.51}{Re_v \sqrt{4f_{vw}}} + \frac{\text{roughness}}{3.7D} \right), \quad (17)$$

$$(3) \quad 1000 < Re_v < 4000$$

$$f_{vw} = f_{vw}(1000) + \frac{f_{vw}(4000) - f_{vw}(1000)}{4000 - 1000} (Re_v - 1000)$$

where

$$Re_v = \frac{\rho_v U_v 2\delta}{\mu_v}.$$

#### 2.2.4 Interfacial shear stresses

It is assumed that interfacial shear stresses of vapour and liquid phases are equal as follows:

$$\tau_{vi} = -\tau_{li} \quad (18)$$

and  $\tau_{vi}$  is defined as

$$\tau_{vi} = \frac{1}{2} f_{vi} \rho_v |U_v - U_i| (U_v - U_i), \quad (19)$$

where  $f_{vi}$  is the interfacial friction factor. It is difficult to determine  $f_{vi}$ , because it is affected by some factors such as interfacial disturbance. Thus, a general correlation of  $f_{vi}$  appropriate for IAFB is lacking. We assume that the wavy interfacial friction factor is made up of the smooth interfacial friction factor and the interfacial disturbance factor. In other words, the interface is rough due to the disturbance. We use Aritomi's empirical correlation<sup>[25]</sup>:

$$f_{vi} = \frac{0.0791}{Re_i^{0.25}} F \quad (20)$$

where

$$F = 1 + 90.9 \frac{\delta}{D_i} \quad \text{and} \quad (21)$$

$$Re_i = \frac{\rho_v (U_v - U_i) D_i}{\mu_v}.$$

In above relation,  $(0.0791/Re_i^{0.25})$  is the friction factor of smooth interface <sup>(25)</sup> and  $F$  is the wavy interface influence factor <sup>(22)</sup> accounting for the effect of interfacial disturbance. The interfacial disturbance is enhanced and the interface becomes more non-smooth with increase of vapour void fraction <sup>(26)</sup>.

## 2.2.5 Heat transfers of vapour phase

The mechanism of heat transfer in IAFB is not well understood at present<sup>(27)</sup>. The vapour is, for example, treated as a flow between two parallel plates; one is the wall and the other is the interface <sup>(14,15)</sup>. This hypothesis is, however, not correct according to the observation by Costigan and Wade <sup>(28)</sup>. In this study, the hypothesis of annular vapour film which may be better approach to the real flow has been proposed in the Sec. 2.2.1 .

For fluid flowing in an annular tube, the heat flux of inner and outer tube have been derived by M.W.Kays <sup>(29)</sup> and are given by

$$q_{ow} = H_{ow}(T_w - T_v) = \frac{k_v}{Dh} \cdot \frac{Nu_w}{1 - \frac{q_{vi}}{q_{vw}} \theta_w} (T_w - T_v) , \quad (22)$$

$$q_{vi} = H_{vi}(T_v - T_s) = \frac{k_v}{Dh} \cdot \frac{Nu_i}{1 - \frac{q_{vw}}{q_{vi}} \theta_i} (T_v - T_s) . \quad (23)$$

where  $Nu_i$  is defined as the inner-tube Nusselt number when the inner tube alone is heated and  $Nu_w$  is outer-tube Nusselt number when the outer tube alone is heated. The parameters  $\theta_w$  and  $\theta_i$  are influence coefficients. We assume that the interface is at the saturation temperature,  $T_s$ , in above equations.

From Eqs.(22) and (23), we can obtain

$$H_{vi} = \frac{1 + Nu^* B \theta_i}{Nu^* + \frac{\theta_w}{B}} H_{ow} , \quad (24)$$

where

$$B = \frac{T_w - T_v}{T_v - T_s} \text{ and } Nu^* = \frac{Nu_w}{Nu_i} .$$

For laminar flow, constants in above correlations (  $Nu_w$ ,  $Nu_i$ ,  $\theta_w$  and  $\theta_i$  ) are given by Kays <sup>(29)</sup> and are listed in Table 2.1.

Here we use the empirical correlation of wall heat transfer coefficient from Aritomi's test <sup>(22)</sup> and the above relation of heat transfer coefficients for  $H_{vw}$  and  $H_{vi}$ . Aritomi's empirical correlation of  $H_{vw}$  is

$$H_{vw} = \frac{2k_v}{\delta} (1 + 90.9 \frac{\delta}{D}) . \quad (25)$$

In Eq.(25), we can find that the  $H_{vw}$  includes the laminar heat transfer coefficient,  $2k_v/\delta$ , and the wavy interface influence factor,  $F$ . This implies that the disturbance of interface enhances the wall heat transfer.

#### 2.2.6 Heat transfers of liquid phase

If liquid phase is not in touch with the wall, heat transfer between liquid and wall is only the radiation heat transfer. The radiation heat flux,  $q_{rad}$ , is given by

$$q_{rad} = \frac{\sigma_B (T_w^4 - T_s^4)}{\frac{1}{\epsilon_w} + \frac{1}{\epsilon_l} - 1} \quad (26)$$

where  $\sigma_B$  is the Stefan-Boltzmann constant and  $\epsilon$  is the emissivity.

The heat from the vapour to the interface is assumed to be used for vaporization of liquid and increase of subcooled liquid temperature. The heat flux from the liquid interface to the bulk of liquid can be expressed by

$$q_{li} = H_{li} (T_s - T_l)$$

where

$$H_{li} = 1287.0 \times \{ 1 + 0.8 \times (T_s - T_l) U_i^{1.5} \frac{\delta}{D_i} \} . \quad (27)$$



The above relation is an empirical correlation from Aritomi <sup>(22)</sup> who took into account the effect of liquid subcooling, liquid velocity and interfacial disturbance on heat transfer.

### 2.2.7 Mass transfer rate

The mass transfer rates at the interface,  $\Gamma_{vi}$  and  $\Gamma_{li}$ , are obtained as follows:

$$\Gamma_{vi} = -\Gamma_{li} = -\frac{q_{vi} + q_{li}}{h_{vs} - h_{ls}}, \quad (28)$$

where  $h_{vs}$  and  $h_{ls}$  are the saturated enthalpies of vapour and liquid, respectively.

Table 2.1 The Influence Coefficient<sup>[29]</sup>

$r_i = r_w^{-1}$	$Nu_i$	$Nu_w$	$\theta_i$	$\theta_w$
0.0	$\infty$	4.364	$\infty$	0.0
0.05	17.81	4.792	2.18	0.0294
0.10	11.91	4.834	1.383	0.0562
0.20	8.499	4.883	0.905	0.1041
0.40	6.583	4.979	0.603	0.1823
0.60	5.912	5.099	0.473	0.2455
0.80	5.580	5.240	0.401	0.2990
1.00	5.385	5.385	0.346	0.346

### 3. Calculated results and discussion

To assess the predictive capabilities and limitations of the present model, we chose a number of cases covering a wide range of different parameters from the experimental data by Aritomi <sup>[22]</sup> and Stewart <sup>[18]</sup>. The hydrodynamic conservation equations together with the constitutive relations are solved by using MINCS from JAERI.

MINCS is designed to analyse transient two-phase flow in one-dimensional ducts. Nine types of two-phase flow model are prepared from the two-fluid non-equilibrium (2V2T) model to the homogeneous equilibrium (1V1T) model. A fully-implicit finite difference scheme with the staggered mesh in space is used. The Newton method is used to solve the discretized equations. In this work, we use 2V2T model. The constitutive relations for IAFB are implemented into subroutine CORSET. Physical properties of Freon-113 are also implemented into subroutine STEAM2 and are listed in Appendix B.

#### 3.1 Comparison with Aritomi's experiment

##### 3.1.1 Description of experiment

In Aritomi's test, the hot patch <sup>[30]</sup> was used to generate the IAFB regime in a vertical tube made of stainless steel and Freon-113 was used as the test fluid. In the experiment, the wall temperature distribution of the test section, fluid temperatures at inlet and outlet, the pressure drop and the vapour film thickness were measured. Experimental conditions are summarized as follows:

Test fluid	: Freon-113
System pressure	: Atmospheric pressure
Inlet velocity	: 0.5 -- 2.0 m/sec
Heated flux	: 20 -- 50 $kw/m^2$
Wall temperature	: 150 -- 300 °C
Inlet subcooling	: 10.7, 15.7, 20.7 K
Heat length	: 100, 300, 500 mm
Test tube - I.D.	: 9.8 mm
Test tube - O.D.	: 10.0 mm

Hot patch length : 5.0 mm

### 3.1.2 Result and discussion

All steady state results for IAFB are calculated by using a time marching method in which the steady state is obtained by a transient solution under constant boundary conditions with time. The input model and input data are listed in Appendix A. The hot patch is treated as a tube with constant wall temperature which is higher than the minimum stable film boiling temperature. Thus, film boiling occurs at the hot patch.

The typical results with 1.5 m/s inlet velocity, 40 kw/m<sup>2</sup> heat flux and 10.7 K subcooling are shown in Fig.3.1. The void fraction is shown in Fig.3.1(a), temperatures of gas, liquid, saturation and wall are in Fig.3.1(b), velocities of both phases in Fig.3.1(c) and heat transfer coefficients of wall and interface in Fig.3.1(d) respectively. Fig. 3.1(a) shows that the void fraction increases along the channel, which agrees well with the experimental result. It is shown in Fig.3.1(b) that the vapour phase is superheated and liquid phase is subcooled. The velocity of vapour phase increases quickly at upstream and is far larger than that of liquid as shown in Fig.3.1(c). The heat transfer coefficients are very large near the inlet where the void fraction is small and the vapour temperature is increasing. They are about the constant values in the downstream as shown in Fig.3.1(d), where the void fraction is large and the vapour temperature does not change largely. This tendency is resulted from the empirical correlation defined by Eq.(25).

## 3.2 Comparison with Stewart's experiment

### 3.2.1 Description of Stewart's experiment

The experimental data for stable film boiling by Stewart using water were published in 1981<sup>(18)</sup>. These data were obtained in an 8.9 mm ID Inconel-600 tube at low-quality and subcooled condition, a mass flux range of 110 to 2750 kg/(m<sup>2</sup>.sec) and pressure from 2 to 9 MPa by using the hot patch technique. In this experiment, axial wall temperatures, fluid temperatures at inlet and outlet and pressure difference between inlet and outlet were measured. The length of vertical test section was 1.8 m. Only a part of experimental data listed

in Table 3.1 is compared with calculated result.

### 3.2.2 Result and discussion

Calculated void fraction and wall temperature are shown in Fig. 3.2. The void fraction smoothly increases along the test section from the inlet to about 0.8 m (including hot patch), but it becomes oscillatory at the downstream as shown in Fig.3.2(a). Figure 3.2(a) shows the void fraction profile at a certain time step. The void fractions near the inlet could be at the steady state in all cases, however, stable results of void fraction and velocities at the downstream could not be obtained. The wall temperature, however, is in the steady state and in reasonable agreement with the experimental result even in the downstream as seen in Fig.3.2(b). These results may indicate that the present model can not be applied to the downstream since the Aritomi's empirical correlations are based on the experiment with short-length test section. That is, the present model may be appropriate only to the range of low void fraction. As for the Stewart's experiment, however, the flow regime at the downstream might not be in the steady IAFB condition. It is very difficult to judge whether IAFB occurred or not in the full test section in Stewart's experiment since a very long opaque tube of Inconel-600 was used as the test section and neither void fraction nor velocities was not measured. In this study, as we take interest only in IAFB problem, the flow region up to 0.6 m of the test section is considered in the following.

The comparisons of wall temperature between calculated and experimental results under different pressures are shown in Fig.3.3(a) to Fig.3.3(d). We can find that the difference between calculated result and experimental data is small for low pressure condition, but become larger with the increase of pressure. The reason for this difference is probably related to the fact that the present model are based on some empirical correlations at atmospheric pressure, for example,  $H_{vw}$ . The trend of the calculated results, however, is in reasonable agreement with experimental data. At pressure of 2 MPa, the difference between the calculated and measured wall temperatures is within the range of 10% in all run analysed. Thus, we can conclude that the present model is appropriate to IAFB in the low pressure range and the pressure dependency should be included in the heat transfer coefficients for the

wide range of application.

It is shown in Fig. 3.4 that the effect of hot patch on IAFB is large in this experiment. The void fraction and vapour velocity at the exit of the hot patch become large due to the large heat flux from the hot patch to fluid.

The calculated temperatures of wall, vapour, liquid and saturation are shown in Fig.3.5. It is found that the vapour phase is superheated and liquid phase is subcooled. The vapour superheat phenomenon in IAFB region has been observed in many experiments, for example, measurements of vapour temperature by Nijhawan et al <sup>[31]</sup>. They showed that the vapour superheat was a significant fraction of the wall superheat (approximately 60%). In our results shown in Fig.3.5, the vapour superheat is about 65% of the wall superheat.

The effects of inlet velocity, subcooling and system pressure on the wall heat transfer coefficient are shown in Figs.3.6, 3.7 and 3.8, respectively. It is found that the wall heat transfer coefficient increases as these parameters increase. In Ref. [18], wall heat transfer coefficients were obtained simply based on the wall heat flux, the wall temperature and the saturation temperature according to the outlet pressure. Thus, the direct comparison is difficult, however, the same trends of these effects were also found in experimental results.

Table 3.1 Test Cases Chosen from Stewart's Test<sup>[18]</sup>

Run number	Pressure KPa	Velocity M.Sec <sup>-1</sup>	Subcooling K	Heat flux KW.M <sup>-2</sup>
2211.02	2032	0.248	16.4	117.7
2321.06	2025	0.401	27.8	122.1
2411.02	1982	0.597	15.4	202.3
2411.04	2040	0.600	14.5	156.4
2411.06	2003	0.600	14.7	112.4
2411.09	2036	0.600	14.7	88.11
2511.07	2049	1.051	13.4	117.9
4311.07	4096	0.631	16.4	124.6
4411.04	4044	0.632	14.9	191.9
4411.06	4076	0.635	14.1	141.3
4411.09	4072	0.636	14.4	119.9
4421.05	4123	0.616	25.4	197.6
6421.04	6006	0.660	24.2	211.4
6421.05	5998	0.660	23.9	182.0
6431.04	6003	0.643	39.7	235.5
8421.04	8008	0.683	22.1	205.3
8421.07	7986	0.685	22.4	159.6

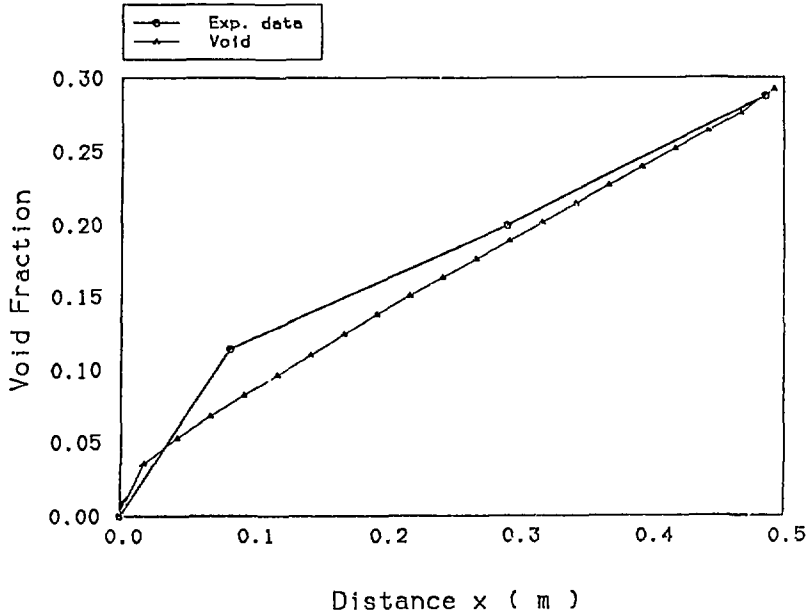


Fig. 3.1(a) (Typical Run.) Void Fraction

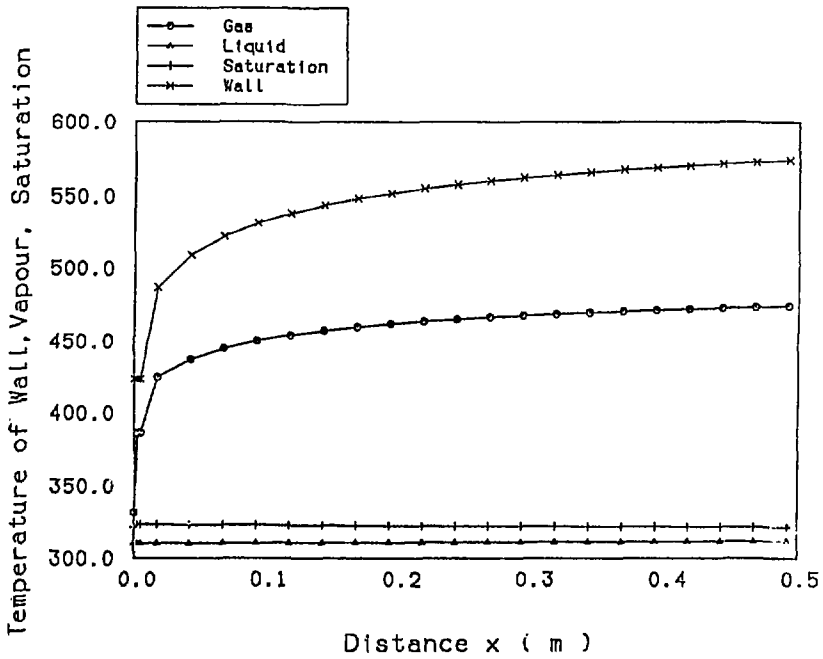


Fig. 3.1(b) (Typical Run.) Temp. of Wall, Vapour, Saturation, Liquid

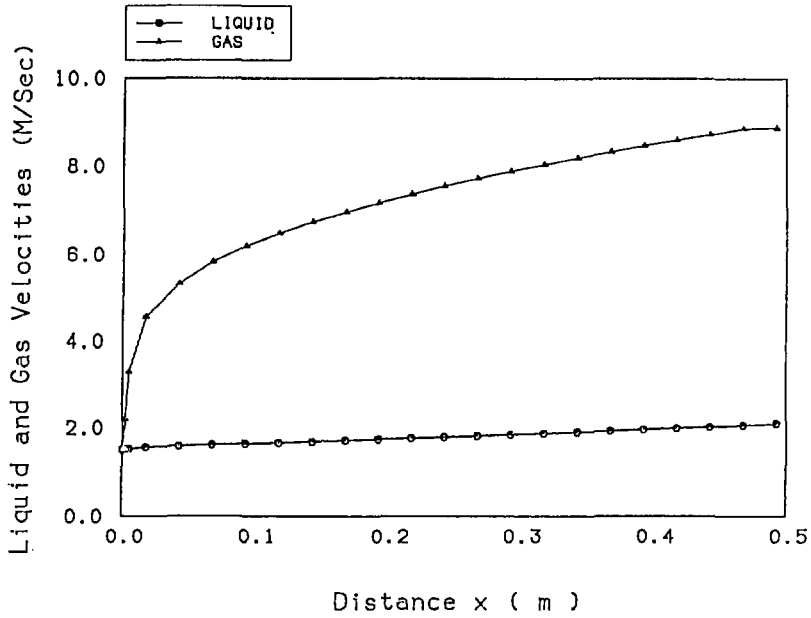


Fig. 3.1(c) (Typical Run.) Liquid and Gas Velocities

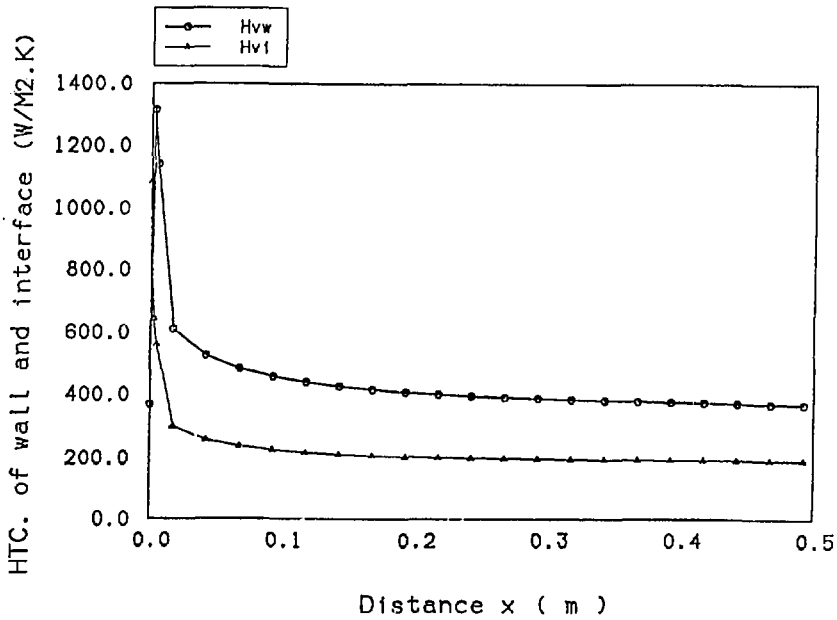


Fig. 3.1(d) (Typical Run.) HTC. of wall and interface



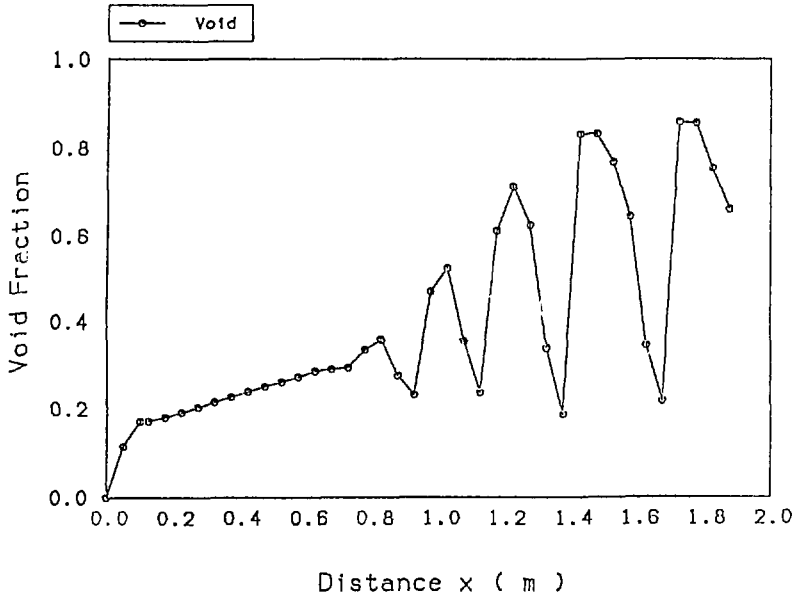


Fig. 3.2(a) (Run. 2411.06.) Void Fraction

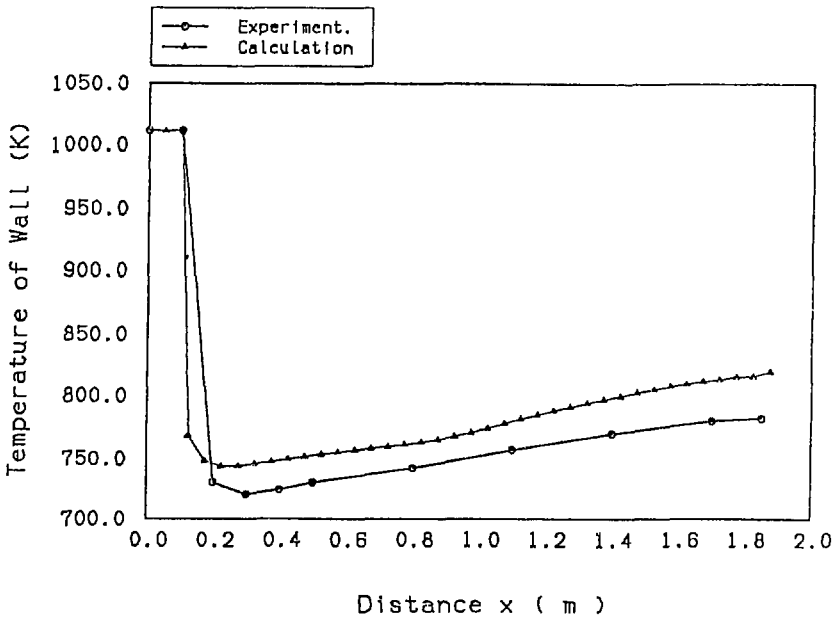


Fig. 3.2(b) (Run. 2411.06.) Wall Temperature (K)

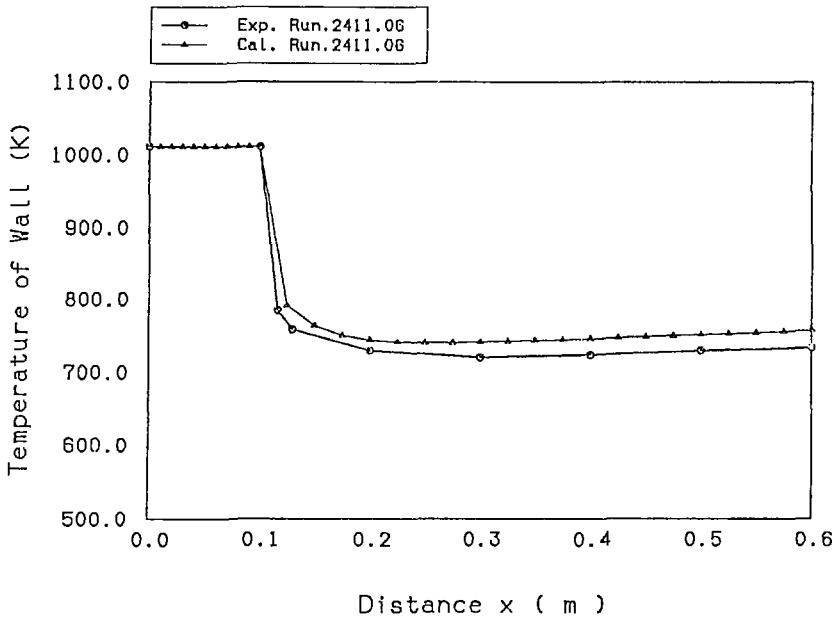


Fig. 3.3(a) (P. 2 MPa.) Comparison of Wall Temperature (K)

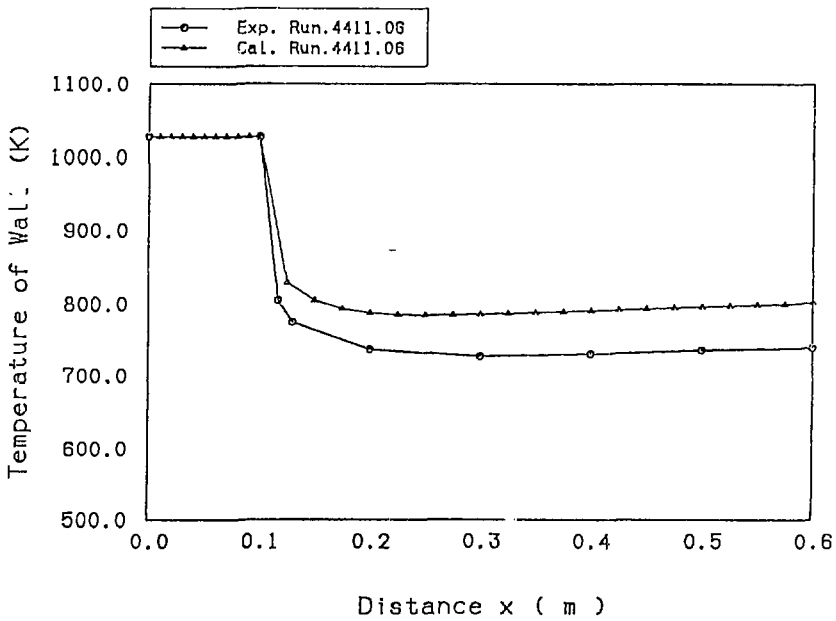


Fig. 3.3(b) (P. 4 MPa.) Comparison of Wall Temperature (K)

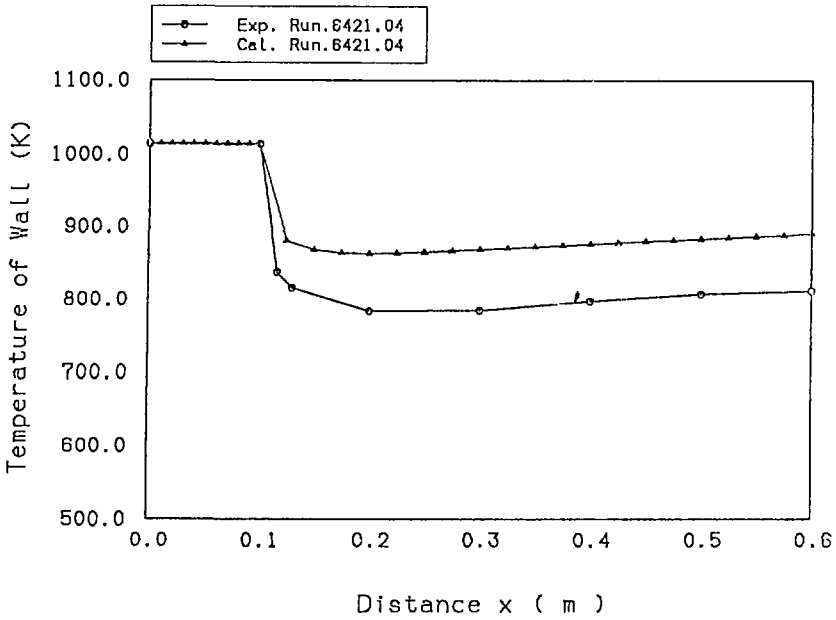


Fig. 3.3(c) (P. 6 MPa.) Comparison of Wall Temperature (K)

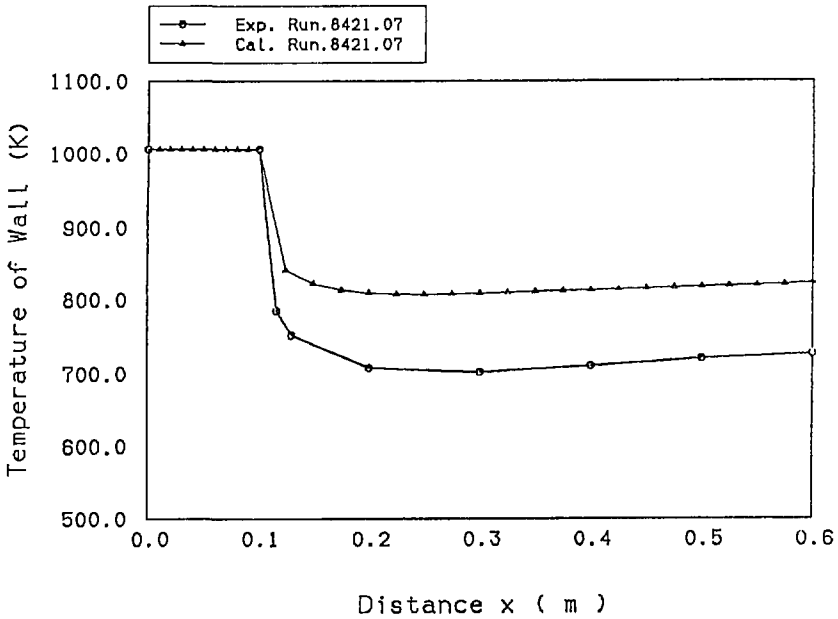


Fig. 3.3(d) (P. 8 MPa.) Comparison of Wall Temperature (K)

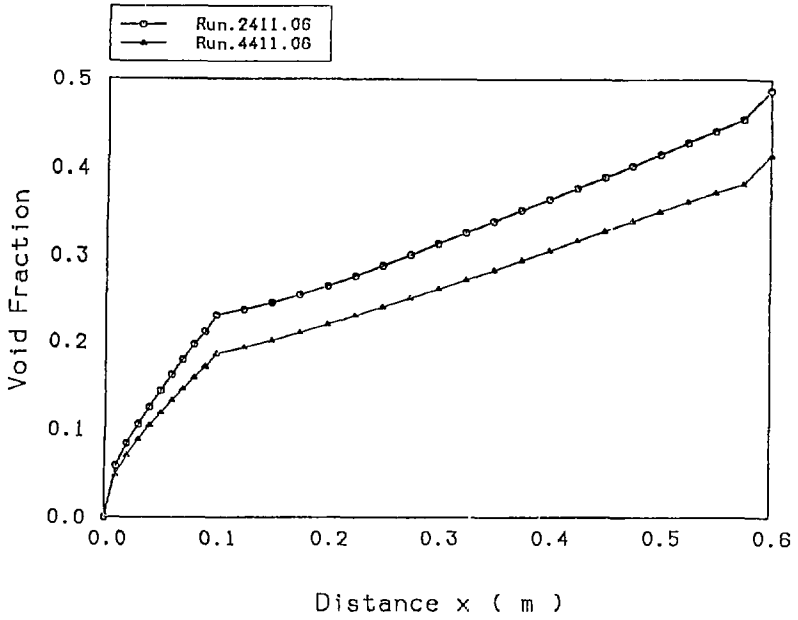


Fig. 3.4(a) Void Fraction

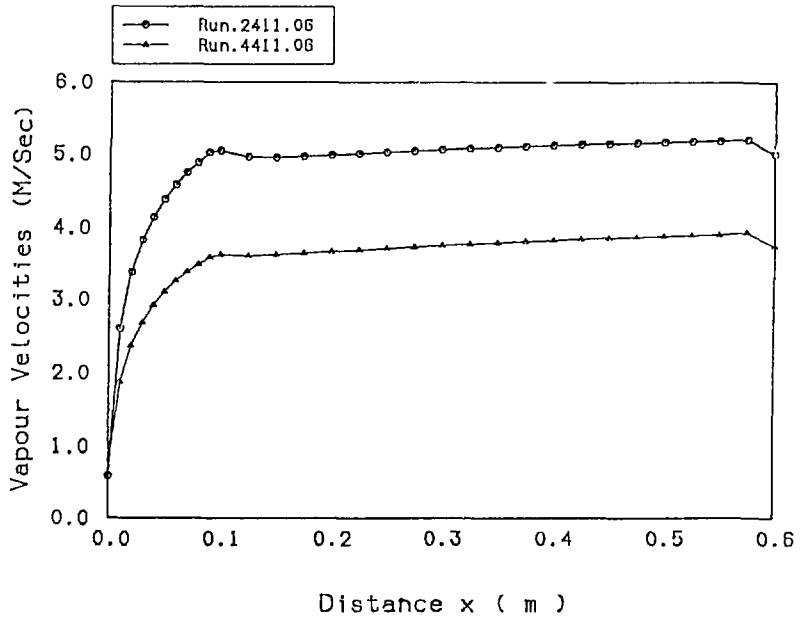


Fig. 3.4(b) Vapour Velocity

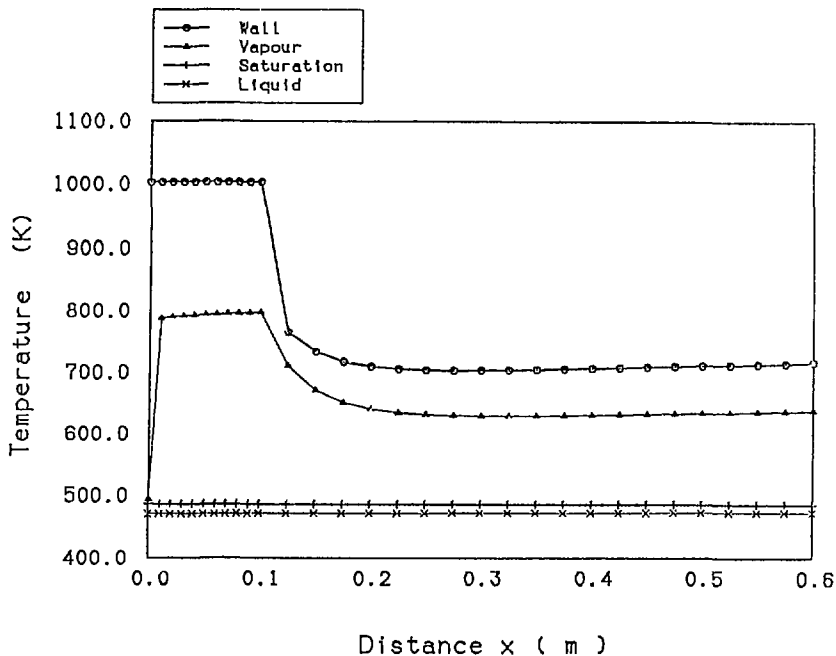


Fig. 3.5(a) (Run. 2411.09.) Temp. of Wall, Vapour, Liquid and Sat.

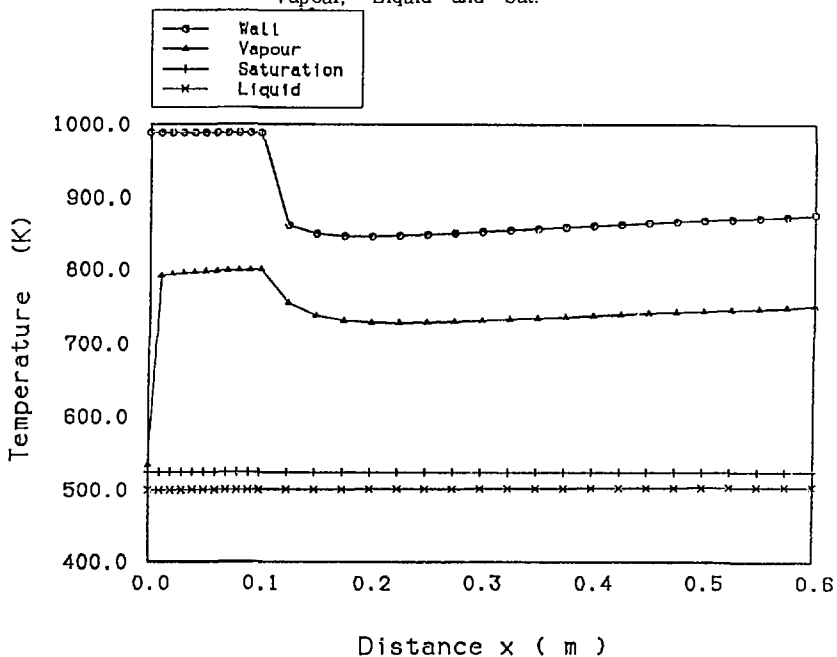


Fig. 3.5(b) (Run. 4421.05.) Temp. of Wall, Vapour, Liquid and Sat.

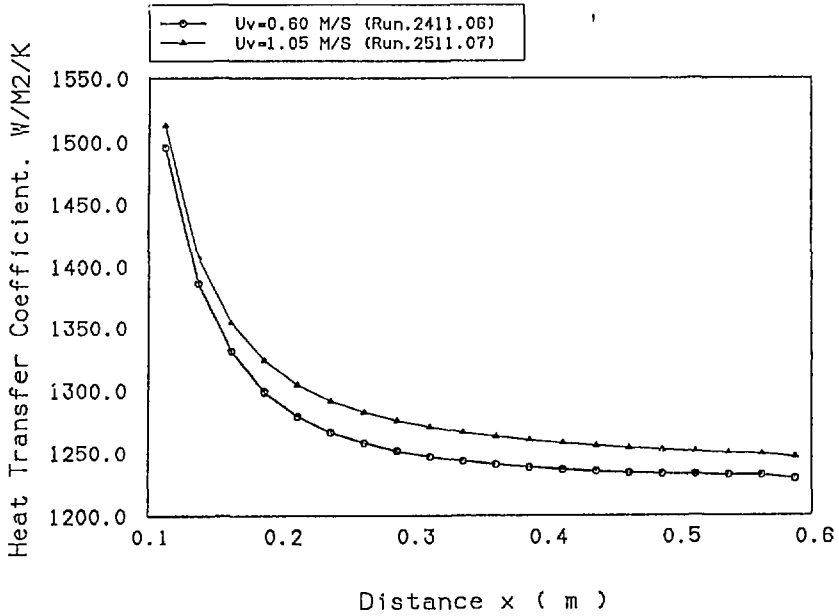


Fig. 3.6 The Effect of Velocity on Heat Transfer Coefficient.

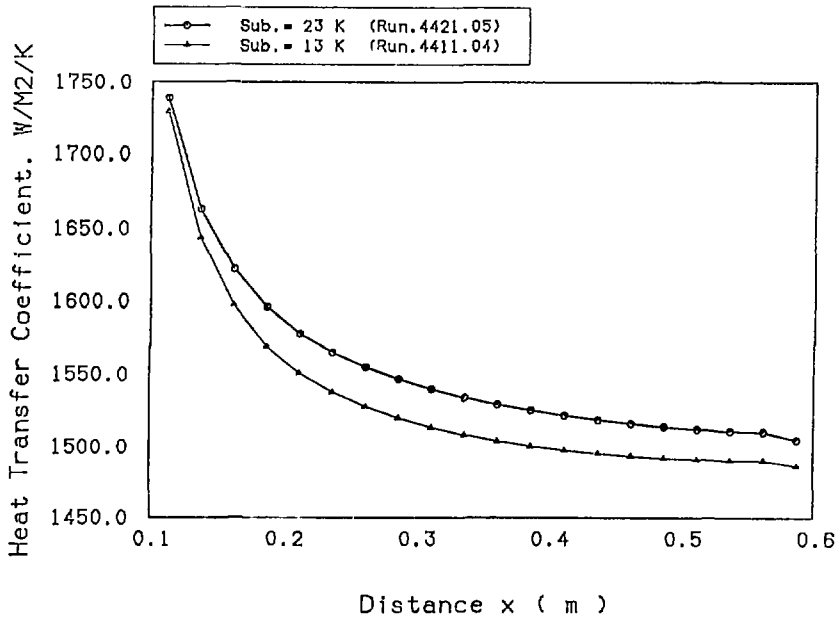


Fig. 3.7 The Effect of Subcooling on Heat Transfer Coefficient

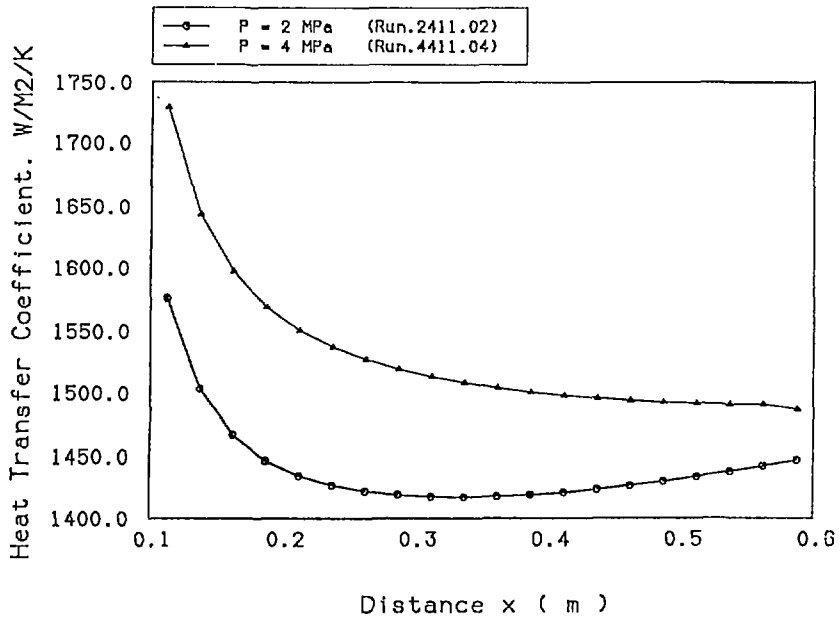


Fig. 3.8 The Effect of Pressure on Heat Transfer Coefficient.

#### 4. Summary and conclusion

The inverted annular film boiling phenomena have gradually been understood, but there are still unknown problems, particularly in the hydrodynamic aspect. The development of two-fluid model of IAFB makes it possible to analyse IAFB in detail, but the information about interactions of two phases are needed. In this work, the two-fluid model in MINCS was used for the analysis of IAFB. By analysis of the Aritomi's IAFB tests, a set of new constitutive relations appropriate to IAFB were proposed. The proposed model were applied to the analysis of Stewart's experiment for verification.

In our model, we assumed the vapour phase as the flow in an annular channel where outside was the tube wall and inside was the interface of liquid-vapour. We obtained the heat transfer coefficient of wall-vapour, vapour-interface and interface-liquid based on above assumption and Aritomi's empirical correlation of wall heat transfer coefficient. The assumption we used is different from the former simple one, for example, by M.Kawaji and G.Th.Analytis who treated the vapour as the flow between two parallel flat plates.

The fact that the interface of liquid-vapour is non-smooth was considered in this work. The interfacial friction and the heat flux from the vapour to the liquid would be enhanced due to interfacial disturbance. An interfacial influence factor which was derived from Aritomi's experiment was used.

Wall temperature and void fraction predicted by the present model were compared with experimental data from Aritomi's experiment using Freon-113 and very good agreement was obtained. Then, the present model was used to analyse Stewart's experiment using water at a large pressure range from 2 MPa to 9 MPa. This result showed that the right trend of effects of subcooling, velocity and pressure on wall heat transfer coefficient could be obtained. The calculated liquid temperatures were in good agreement with the experimental data. By comparing the calculated wall temperature with experimental data, the better agreement was found to be obtained at low pressure, but the agreement became poor with the increase in pressure.

It is concluded that the present model is appropriate for analysing the IAFB phenomena under such low pressure condition as atmospheric



pressure. The dependence on the pressure, however, should be included for the wide range of its application. Thus, further research on IAFB problem is still necessary, for example, the effect of pressure on the heat transfer coefficient, the effect of interfacial disturbance on friction and heat transfer, and so on.

#### Acknowledgement

I wish to express the deepest gratitude for Japan Atomic Energy Research Institute for submitting this research chance to me. I thank Prof. M.Aritomi of Tokyo Institute of Technology for supplying experimental data of inverted annular film boiling. The advice and help on selection of research subject and plan from Dr. A.Kohsaka, Head of Reactor Safety Evaluation Laboratory in JAERI, are gratefully acknowledged.

## References

- [1] D.D. Taylor, et al., TRAC-BD1/MOD1: An advanced best estimate computer program for boiling water reactor transient analysis, NUREG/CR-3633, EGG-2294 (1984)
- [2] Safety Code Development Group, TRAC-PF1/MOD1: An advanced best estimate computer program for pressurized water reactor thermal-hydraulic analysis, NUREG/CR-3858, LA-10157-MS
- [3] V.H. Ransom, et al., RELAP5/MOD1 code description, NURCG/CR-1826, EGG-2070 (1982)
- [4] M. Akimoto, et al., Development of two-phase flow analyzer: MINCS, 2nd Int. topical mtg. on power plant thermal-hydraulics and operation, 72-79.
- [5] M. Akimoto, et al., MINCS: A computer code for transient thermal-hydraulic analysis in a light water reactor system - MINCS-PIPE: A computer code for transient two-phase flow analysis in one-dimension ducts (in Japanese), JAERI-M84-202.
- [6] M. Ishii and G. Dejarlais, Flow visualization study of inverted annular flow of post dryout heat transfer region, Nucl. Eng. Des. 99(1987) 187-199
- [7] G.E. Coury and A.E. Dukler, Turbulent film boiling on vertical surface - A study including the influence of interfacial waves, Proc. Int. Heat Transfer Conf., Paris (1970).
- [8] N.V. Suryanarayana and H. Merte Jr., Film boiling on vertical surface, Trans. ASME., J. Heat transfer 94(1972) 377-384.
- [9] Z. Edelman, D. Naot and E. Elias, Optical illustration of liquid penetration to vapour film in inverted annular boiling, Int. J. Heat Mass Transfer 26(1983) 1715-1717.
- [10] D.C. Groeneveld, Inverted annular and low quality film boiling: A state-of-the-art report, Intern. Workshop on Fundamental aspects of Post-dryout Heat Transfer (1984), Salt Lake City, Utah, USA.
- [11] R.S. Dougall and W.M. Rohsenow, Film boiling on the inside of vertical tubes with upward flow of the fluid at low qualities, MIT report 9079-26 (1963)
- [12] E. Elias and P. Chambre, Inverted annular film boiling heat transfer from vertical surface, Nucl. Eng. Des. 64 (1981) 249-257.

- [13] M. Osakabe and Y. Sudo, Analysis of saturated film boiling heat transfer in reflood phase of LOCA, J. Nucl. Sci. Techn. 21 (1984) 115-125.
- [14] M. Kawaji and S. Banerjee, A two-fluid model for reflooding of a vertical tube: structure and stability of the inverted annular flow model, The 21st ASME-AIChE National Heat Transfer Conference.
- [15] G.Th. Analytis and G. Yadigaroglu, Analytical modeling of inverted annular film boiling, Nucl. Eng. Des. 99 (1987) 201-212.
- [16] J.M. Kaufman and P. Griffith, Post critical heat flux heat transfer to water in a vertical tube, USNRC Report NURCG-0164 (1977).
- [17] K.K. Fung, S.R.M. Gardner and D.C. Groeneveld, Subcooled and low quality flow film boiling of water at atmospheric pressure, Nucl. Eng. Des. 55(1979) 51-57.
- [18] J.C. Stewart and D.C. Groeneveld, Low-quality and subcooled flow film boiling of water at elevated pressure, Nucl. Eng. Des. 67(1981) 259-272.
- [19] H. Bi, J. Xu, Z. Guo and K. Wang , et al, Low quality and subcooled inverted-annular flow film boiling of water at low pressure (In Chinese), Nucl. Power Eng. V. 7(4) p.28-35.
- [20] D.C. Groeneveld and S.R.M. Gardiner, Post CHF heat transfer under force convective conditions, Proc. Symp. on the Thermal and Hydraulic Aspects of Nuci. Reactors safety, New York, ASME 1 (1977) p.43.
- [21] D.C. Groeneveld, Post dryout heat transfer: Physical mechanics and a survey of prediction methods, Nucl. Eng. Des. 32(1975) 283.
- [22] M. Aritomi, et al, Thermal and hydraulic behavior of inverted annular flow, 2nd Int. topical mtg. on power plant thermal-hydraulics and operation, April 1986, Tokyo, Japan, 1-34 - 1-42.
- [23] L. Bromley, Heat Transfer in stable film boiling, Chem. Eng. Prog. Vol.46 (1950), pp. 221-227.
- [24] R.W. Lockhart and R.C. Martinell, Proposed correlation of data for isothermal two-phase, two-component flow in pipes . , Chem. Eng. Prog. , Vol.45(1), pp. 39-48, 1949.
- [25] M. Takahashi, M. Aritomi, A. Inoue and S. Aoki, Interface turbulent heat transfer of horizontal co-current liquid-liquid stratified flow (3rd. Boiling in water), 17th Nat. Heat Transfer Symp. Japan, pp.220-222, 1980.

- [26] G.De. Jarlais, An experimental study of inverted annular flow hydrodynamics utilizing an adiabatic simulation, NUREG/CR-3339, ANL-83-44
- [27] M. Ishii and G.De. Jarlais, Flow regime transition and interfacial characteristics of inverted annular flow, Nucl. Eng. and Des. 95 (1986) 171-184
- [28] G. Costigan and C.D. Wade, Visualization of the reflooding of a vertical tube by dynamic neutron radiography, Int. Workshop on Post-dryout Heat Transfer (1984), Salt Lake City, Utah, USA.
- [29] W.M. Kays, Convective heat transfer, Mc-Graw-Hill Book Company, New York, 1966.
- [30] D.C. Groeneveld and S.R.M. Gardiner, A method of obtaining flow film boiling data for subcooled water, Int. J. Heat Mass Transfer 21 (1978) 17-26.
- [31] S. Nijhawan et al., Measurement of vapour superheat in post-critical heat flux boiling, ASME J. Heat Transfer 102 (1980) 450-470.

## Appendix A Input model of MINCS for IAFB

In the calculation of IAFB by MINCS, the following model shown in Fig.A-1 is used to simulate test facilities of M.Aritomi and J.C.Stewart. In Fig.A-1, Boundary-L and Boundary-R denote inlet and exit of test tube. Pipe-1 and Pipe-2 are the hot patch and the test section. Heat slabs of the hot patch are treated as constant temperature, because their quantities of heat capacity are very large. Input data of MINCS for Aritomi's and Stewart's tests are listed in Appendix A.1 and A.2.

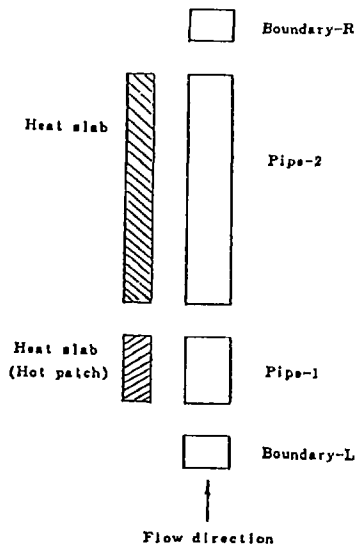


Fig. A-1 Input model for IAFB

## Appendix A.1 Input Data For Aritomi's Experiment.

```

JAFB ANALYSIS FOR FREON-113
0 0
0
0 1 2
7.3833 6.8839D-5 1510.5 1.0D-10 1.01325D5 6.0819D5 4.6143D5
4 4 0 22 22 0 0 0 12 1
10 0 0.1 0.1 1.0
0
1.0
0.0
0.01 0.01 30.0 0
500 0 200 0 0 0
14
2
183.15 8.96D3 2356.15 8.35D3
2
173.15 3.85D30 2000.0 3.85D30
5
200.0 413.0 400.0 393.0 500.0 386.0 600.0 379.0 2800.0 366.0
3
100.0 0.50 800.0 0.58 2000.0 0.80
BOUNDARY-L -2 2 2
2 8*0
0 0 0
1 0 1 0 5
1 0 0 0 0 0 7.543D-5 0.10 7.543D-5 0.10 9.8D-3 9.8D-3 0.0
1 1.0D-4 1.01325D5 6.1819D5 4.5144D5 1.50 1.50 0.0 0.0
PIPE1 1 2 2
2 0 0
0 0 0
1 0 1 0 5
1 0 0 0 0 1 7.543D-5 2.5D-3 7.543D-5 2.5D-3 9.8D-3 9.8D-3 0.0
2 0 0 0 0 2 7.543D-5 2.5D-3 7.543D-5 2.5D-3 9.8D-3 9.8D-3 0.0
1 1.0D-2 1.01325D5 6.1819D5 4.5144D5 1.50 1.50 0.0 0.0
2 1.0D-2 1.01325D5 6.1819D5 4.5144D5 1.50 1.50 0.0 0.0
PIPE2 1 2 2
20 0 0
0 0 0
1 0 1 0 5
1 0 0 0 0 1 7.543D-5 2.5D-2 7.543D-5 2.5D-2 9.8D-3 9.8D-3 0.0
2 0 0 0 0 2 7.543D-5 2.5D-2 7.543D-5 2.5D-2 9.8D-3 9.8D-3 0.0
3 0 0 0 0 3 7.543D-5 2.5D-2 7.543D-5 2.5D-2 9.8D-3 9.8D-3 0.0
4 0 0 0 0 4 7.543D-5 2.5D-2 7.543D-5 2.5D-2 9.8D-3 9.8D-3 0.0
5 0 0 0 0 5 7.543D-5 2.5D-2 7.543D-5 2.5D-2 9.8D-3 9.8D-3 0.0
6 0 0 0 0 6 7.543D-5 2.5D-2 7.543D-5 2.5D-2 9.8D-3 9.8D-3 0.0
7 0 0 0 0 7 7.543D-5 2.5D-2 7.543D-5 2.5D-2 9.8D-3 9.8D-3 0.0
8 0 0 0 0 8 7.543D-5 2.5D-2 7.543D-5 2.5D-2 9.8D-3 9.8D-3 0.0
9 0 0 0 0 9 7.543D-5 2.5D-2 7.543D-5 2.5D-2 9.8D-3 9.8D-3 0.0
10 0 0 0 0 10 7.543D-5 2.5D-2 7.543D-5 2.5D-2 9.8D-3 9.8D-3 0.0
11 0 0 0 0 11 7.543D-5 2.5D-2 7.543D-5 2.5D-2 9.8D-3 9.8D-3 0.0

```

```

12 0 0 0 0 12 7.543D-5 2.5D-2 7.543D-5 2.5D-2 9.8D-3 9.8D-3 0.0
13 0 0 0 0 13 7.543D-5 2.5D-2 7.543D-5 2.5D-2 9.8D-3 9.8D-3 0.0
14 0 0 0 0 14 7.543D-5 2.5D-2 7.543D-5 2.5D-2 9.8D-3 9.8D-3 0.0
15 0 0 0 0 15 7.543D-5 2.5D-2 7.543D-5 2.5D-2 9.8D-3 9.8D-3 0.0
16 0 0 0 0 16 7.543D-5 2.5D-2 7.543D-5 2.5D-2 9.8D-3 9.8D-3 0.0
17 0 0 0 0 17 7.543D-5 2.5D-2 7.543D-5 2.5D-2 9.8D-3 9.8D-3 0.0
18 0 0 0 0 18 7.543D-5 2.5D-2 7.543D-5 2.5D-2 9.8D-3 9.8D-3 0.0
19 0 0 0 0 19 7.543D-5 2.5D-2 7.543D-5 2.5D-2 9.8D-3 9.8D-3 0.0
20 0 0 0 0 20 7.543D-5 2.5D-2 7.543D-5 2.5D-2 9.8D-3 9.8D-3 0.0
 1 1.0D-2 1.01325D5 6.1819D5 4.5144D5 1.50 1.50 0.0 0.0
20 1.0D-2 1.01325D5 6.1819D5 4.5144D5 1.50 1.50 0.0 0.0
BOUNDARY-R -1 2 2
 1 8*0
 0 0 0
 1 0 1 0 5
 1 0 0 0 0 7.543D-5 0.10 7.543D-5 0.10 9.8D-3 9.8D-3 0.0
 1 1.0D-2 1.01325D5 6.1819D5 4.5144D5 1.50 1.50 0.0 0.0
PIPE1 1 2
PIPE2 2 3
BOUNDARY-L 1
BOUNDARY-R 3
 0
 2 5 0 0 0 0
 4 615.75
 0.0 0.0
 0.5 0.2
 1.0 1.0
1000.0 1.0
 5 30.788
 0.0 0.0
 0.5 0.2
 1.0 0.5
 2.0 1.0
1000.0 1.0
HEAT01
 1 5
 2.827D-5
 4.90D-3 16.0D-3 27.0D-3 38.0D-3 49.0D-3 60.0D-3
 5*14
 6*423.15
 5*0.2
HEAT02
 1 5
 2.827D-5
 4.90D-3 16.0D-3 27.0D-3 38.0D-3 49.0D-3 60.0D-3
 5*14
 6*423.15
 5*0.2
HEAT03
 1 5
 7.776D-8
 4.90D-3 4.92D-3 4.94D-3 4.96D-3 4.98D-3 5.00D-3
 5*6
 6*373.15

```

5\*0.2  
 HEAT04  
 1 5  
 7.776D-8  
 4.90D-3 4.92D-3 4.94D-3 4.96D-3 4.98D-3 5.00D-3  
 5\*6  
 6\*373.15  
 5\*0.2  
 HEAT05  
 1 5  
 7.776D-8  
 4.90D-3 4.92D-3 4.94D-3 4.96D-3 4.98D-3 5.00D-3  
 5\*6  
 6\*373.15  
 5\*0.2  
 HEAT06  
 1 5  
 7.776D-8  
 4.90D-3 4.92D-3 4.94D-3 4.96D-3 4.98D-3 5.00D-3  
 5\*6  
 6\*373.15  
 5\*0.2  
 HEAT07  
 1 5  
 7.776D-8  
 4.90D-3 4.92D-3 4.94D-3 4.96D-3 4.98D-3 5.00D-3  
 5\*6  
 6\*373.15  
 5\*0.2  
 HEAT08  
 1 5  
 7.776D-8  
 4.90D-3 4.92D-3 4.94D-3 4.96D-3 4.98D-3 5.00D-3  
 5\*6  
 6\*373.15  
 5\*0.2  
 HEAT09  
 1 5  
 7.776D-8  
 4.90D-3 4.92D-3 4.94D-3 4.96D-3 4.98D-3 5.00D-3  
 5\*6  
 6\*373.15  
 5\*0.2  
 HEAT10  
 1 5  
 7.776D-8  
 4.90D-3 4.92D-3 4.94D-3 4.96D-3 4.98D-3 5.00D-3  
 5\*6  
 6\*373.15  
 5\*0.2  
 HEAT11  
 1 5  
 7.776D-8  
 4.90D-3 4.92D-3 4.94D-3 4.96D-3 4.98D-3 5.00D-3



5\*6  
 6\*373.15  
 5\*0.2  
 HEAT12  
 1 5  
 7.776D-8  
 4.90D-3 4.92D-3 4.94D-3 4.96D-3 4.98D-3 5.00D-3  
 5\*6  
 6\*373.15  
 5\*0.2  
 HEAT13  
 1 5  
 7.776D-8  
 4.90D-3 4.92D-3 4.94D-3 4.96D-3 4.98D-3 5.00D-3  
 5\*6  
 6\*373.15  
 5\*0.2  
 HEAT14  
 1 5  
 7.776D-8  
 4.90D-3 4.92D-3 4.94D-3 4.96D-3 4.98D-3 5.00D-3  
 5\*6  
 6\*373.15  
 5\*0.2  
 HEAT15  
 1 5  
 7.776D-8  
 4.90D-3 4.92D-3 4.94D-3 4.96D-3 4.98D-3 5.00D-3  
 5\*6  
 6\*373.15  
 5\*0.2  
 HEAT16  
 1 5  
 7.776D-8  
 4.90D-3 4.92D-3 4.94D-3 4.96D-3 4.98D-3 5.00D-3  
 5\*6  
 6\*373.15  
 5\*0.2  
 HEAT17  
 1 5  
 7.776D-8  
 4.90D-3 4.92D-3 4.94D-3 4.96D-3 4.98D-3 5.00D-3  
 5\*6  
 6\*373.15  
 5\*0.2  
 HEAT18  
 1 5  
 7.776D-8  
 4.90D-3 4.92D-3 4.94D-3 4.96D-3 4.98D-3 5.00D-3  
 5\*6  
 6\*373.15  
 5\*0.2  
 HEAT19  
 1 5

```

7.776D-8
4.90D-3 4.92D-3 4.94D-3 4.96D-3 4.98D-3 5.00D-3
5*6
6*373.15
5*0.2
HEAT20
1 5
7.776D-8
4.90D-3 4.92D-3 4.94D-3 4.96D-3 4.98D-3 5.00D-3
5*6
6*373.15
5*0.2
HEAT21
1 5
7.776D-8
4.90D-3 4.92D-3 4.94D-3 4.96D-3 4.98D-3 5.00D-3
5*6
6*373.15
5*0.2
HEAT22
1 5
7.776D-8
4.90D-3 4.92D-3 4.94D-3 4.96D-3 4.98D-3 5.00D-3
5*6
6*373.15
5*0.2
HEAT01 1 -10 PIPE1 1 0 0 0
HEAT02 1 -10 PIPE1 2 0 0 0
HEAT03 2 -10 PIPE2 1 0 0 0
HEAT04 2 -10 PIPE2 2 0 0 0
HEAT05 2 -10 PIPE2 3 0 0 0
HEAT06 2 -10 PIPE2 4 0 0 0
HEAT07 2 -10 PIPE2 5 0 0 0
HEAT08 2 -10 PIPE2 6 0 0 0
HEAT09 2 -10 PIPE2 7 0 0 0
HEAT10 2 -10 PIPE2 8 0 0 0
HEAT11 2 -10 PIPE2 9 0 0 0
HEAT12 2 -10 PIPE2 10 0 0 0
HEAT13 2 -10 PIPE2 11 0 0 0
HEAT14 2 -10 PIPE2 12 0 0 0
HEAT15 2 -10 PIPE2 13 0 0 0
HEAT16 2 -10 PIPE2 14 0 0 0
HEAT17 2 -10 PIPE2 15 0 0 0
HEAT18 2 -10 PIPE2 16 0 0 0
HEAT19 2 -10 PIPE2 17 0 0 0
HEAT20 2 -10 PIPE2 18 0 0 0
HEAT21 2 -10 PIPE2 19 0 0 0
HEAT22 2 -10 PIPE2 20 0 0 0

```

Appendix A.2 Input Data for Stewart's Experiment

```

IAFB ANALYSIS FOR WATER (RUN.2411.06)
0 0
0
1 1 0
4 4 0 30 30 0 0 0 12 1
10 0 0.1 0.1 1.0
0
1.0
0.0
0.01 0.01 30.0 0
500 0 200 0 0 0
14
2
183.15 8.96D3 2356.15 8.35D3
2
173.15 3.85D30 2000.0 3.85D30
5
200.0 413.0 400.0 393.0 500.0 386.0 600.0 379.0 2800.0 366.0
3
100.0 0.50 800.0 0.58 2000.0 0.80
BOUNDARY-L -2 2 2
2 8*0
0 0 0
1 0 1 0 5
1 0 0 0 0 6.263D-5 0.05 6.263D-5 0.05 8.93D-3 8.93D-3 0.0
1 1.0D-4 2.003D6 2.8199D6 8.4212D5 0.5996 0.5996 0.0 0.0
PIPE1 1 2 2
10 0 0
0 0 0
1 0 1 0 5
1 0 0 0 0 1 6.263D-5 0.01 6.263D-5 0.01 8.93D-3 8.93D-3 0.0
2 0 0 0 0 2 6.263D-5 0.01 6.263D-5 0.01 8.93D-3 8.93D-3 0.0
3 0 0 0 0 3 6.263D-5 0.01 6.263D-5 0.01 8.93D-3 8.93D-3 0.0
4 0 0 0 0 4 6.263D-5 0.01 6.263D-5 0.01 8.93D-3 8.93D-3 0.0
5 0 0 0 0 5 6.263D-5 0.01 6.263D-5 0.01 8.93D-3 8.93D-3 0.0
6 0 0 0 0 6 6.263D-5 0.01 6.263D-5 0.01 8.93D-3 8.93D-3 0.0
7 0 0 0 0 7 6.263D-5 0.01 6.263D-5 0.01 8.93D-3 8.93D-3 0.0
8 0 0 0 0 8 6.263D-5 0.01 6.263D-5 0.01 8.93D-3 8.93D-3 0.0
9 0 0 0 0 9 6.263D-5 0.01 6.263D-5 0.01 8.93D-3 8.93D-3 0.0
10 0 0 0 0 10 6.263D-5 0.01 6.263D-5 0.01 8.93D-3 8.93D-3 0.0
1 1.0D-2 2.003D6 2.8199D6 8.4232D5 0.5996 0.5996 0.0 0.0
10 1.0D-2 2.003D6 2.8199D6 8.4232D5 0.5996 0.5996 0.0 0.0
PIPE2 1 2 2
20 0 0
0 0 0
1 0 1 0 5
1 0 0 0 0 1 6.263D-5 0.025 6.263D-5 0.025 8.93D-3 8.93D-3 0.0
2 0 0 0 0 2 6.263D-5 0.025 6.263D-5 0.025 8.93D-3 8.93D-3 0.0
3 0 0 0 0 3 6.263D-5 0.025 6.263D-5 0.025 8.93D-3 8.93D-3 0.0
4 0 0 0 0 4 6.263D-5 0.025 6.263D-5 0.025 8.93D-3 8.93D-3 0.0

```

```

5 0 0 0 0 5 6.263D-5 0.025 6.263D-5 0.025 8.93D-3 8.93D-3 0.0
6 0 0 0 0 6 6.263D-5 0.025 6.263D-5 0.025 8.93D-3 8.93D-3 0.0
7 0 0 0 0 7 6.263D-5 0.025 6.263D-5 0.025 8.93D-3 8.93D-3 0.0
8 0 0 0 0 8 6.263D-5 0.025 6.263D-5 0.025 8.93D-3 8.93D-3 0.0
9 0 0 0 0 9 6.263D-5 0.025 6.263D-5 0.025 8.93D-3 8.93D-3 0.0
10 0 0 0 0 10 6.263D-5 0.025 6.263D-5 0.025 8.93D-3 8.93D-3 0.0
11 0 0 0 0 11 6.263D-5 0.025 6.263D-5 0.025 8.93D-3 8.93D-3 0.0
12 0 0 0 0 12 6.263D-5 0.025 6.263D-5 0.025 8.93D-3 8.93D-3 0.0
13 0 0 0 0 13 6.263D-5 0.025 6.263D-5 0.025 8.93D-3 8.93D-3 0.0
14 0 0 0 0 14 6.263D-5 0.025 6.263D-5 0.025 8.93D-3 8.93D-3 0.0
15 0 0 0 0 15 6.263D-5 0.025 6.263D-5 0.025 8.93D-3 8.93D-3 0.0
16 0 0 0 0 16 6.263D-5 0.025 6.263D-5 0.025 8.93D-3 8.93D-3 0.0
17 0 0 0 0 17 6.263D-5 0.025 6.263D-5 0.025 8.93D-3 8.93D-3 0.0
18 0 0 0 0 18 6.263D-5 0.025 6.263D-5 0.025 8.93D-3 8.93D-3 0.0
19 0 0 0 0 19 6.263D-5 0.025 6.263D-5 0.025 8.93D-3 8.93D-3 0.0
20 0 0 0 0 20 6.263D-5 0.025 6.263D-5 0.025 8.93D-3 8.93D-3 0.0
1 1.0D-2 2.003D6 2.8199D6 8.4232D5 0.5996 0.5996 0.0 0.0
20 1.0D-2 2.003D6 2.8199D6 8.4232D5 0.5996 0.5996 0.0 0.0
BOUNDARY-R -1 2 2
1 8*0
0 0 0
1 0 1 0 5
1 0 0 0 0 6.263D-5 0.05 6.263D-5 0.05 8.93D-3 8.93D-3 0.0
1 1.0D-2 1.990D6 2.8199D6 8.2153D5 0.5996 0.5996 0.0 0.0
PIPE1 1 2
PIPE2 2 3
BOUNDARY-L 1
BOUNDARY-R 3
0
2 5 0 0 0 0
4 136.50
0.0 0.0
0.5 0.2
1.0 1.0
1000.0 1.0
5 78.819
0.0 0.0
0.5 0.2
1.0 0.5
2.0 1.0
1000.0 1.0
HEAT01
1 5
7.791D-5
4.465D-3 5.01D-3 5.555D-3 20.0D-3 45.0D-3 50.0D-3
2*12 3*14
6*1011.15
0.0 0.0 0.3333 0.3333 0.3333
HEAT02
1 5
7.791D-5
4.465D-3 5.01D-3 5.555D-3 20.0D-3 45.0D-3 50.0D-3
2*12 3*14
6*1011.15

```

0.0 0.0 0.3333 0.3333 0.3333  
 HEAT03  
 1 5  
 7.791D-5  
 4.465D-3 5.01D-3 5.555D-3 20.0D-3 45.0D-3 50.0D-3  
 2\*12 3\*14  
 6\*1011.15  
 0.0 0.0 0.3333 0.3333 0.3333  
 HEAT04  
 1 5  
 7.791D-5  
 4.465D-3 5.01D-3 5.555D-3 20.0D-3 45.0D-3 50.0D-3  
 2\*12 3\*14  
 6\*1011.15  
 0.0 0.0 0.3333 0.3333 0.3333  
 HEAT05  
 1 5  
 7.791D-5  
 4.465D-3 5.01D-3 5.555D-3 20.0D-3 45.0D-3 50.0D-3  
 2\*12 3\*14  
 6\*1011.15  
 0.0 0.0 0.3333 0.3333 0.3333  
 HEAT06  
 1 5  
 7.791D-5  
 4.465D-3 5.01D-3 5.555D-3 20.0D-3 45.0D-3 50.0D-3  
 2\*12 3\*14  
 6\*1011.15  
 0.0 0.0 0.3333 0.3333 0.3333  
 HEAT07  
 1 5  
 7.791D-5  
 4.465D-3 5.01D-3 5.555D-3 20.0D-3 45.0D-3 50.0D-3  
 2\*12 3\*14  
 6\*1011.15  
 0.0 0.0 0.3333 0.3333 0.3333  
 HEAT08  
 1 5  
 7.791D-5  
 4.465D-3 5.01D-3 5.555D-3 20.0D-3 45.0D-3 50.0D-3  
 2\*12 3\*14  
 6\*1011.15  
 0.0 0.0 0.3333 0.3333 0.3333  
 HEAT09  
 1 5  
 7.791D-5  
 4.465D-3 5.01D-3 5.555D-3 20.0D-3 45.0D-3 50.0D-3  
 2\*12 3\*14  
 6\*1011.15  
 0.0 0.0 0.3333 0.3333 0.3333  
 HEAT10  
 1 5  
 7.791D-5  
 4.465D-3 5.01D-3 5.555D-3 20.0D-3 45.0D-3 50.0D-3

```

2*12 3*14
6*1011.15
0.0 0.0 0.3333 0.3333 0.3333
HEAT11
1 5
0.8678D-6
4.465D-3 4.683D-3 4.901D-3 5.117D-3 5.337D-3 5.555D-3
5*12
6*900.15
5*0.2
HEAT12
1 5
0.8678D-6
4.465D-3 4.683D-3 4.901D-3 5.117D-3 5.337D-3 5.555D-3
5*12
6*900.15
5*0.2
HEAT13
1 5
0.8678D-6
4.465D-3 4.683D-3 4.901D-3 5.117D-3 5.337D-3 5.555D-3
5*12
6*900.15
5*0.2
HEAT14
1 5
0.8678D-6
4.465D-3 4.683D-3 4.901D-3 5.117D-3 5.337D-3 5.555D-3
5*12
6*900.15
5*0.2
HEAT15
1 5
0.8678D-6
4.465D-3 4.683D-3 4.901D-3 5.117D-3 5.337D-3 5.555D-3
5*12
6*900.15
5*0.2
HEAT16
1 5
0.8678D-6
4.465D-3 4.683D-3 4.901D-3 5.117D-3 5.337D-3 5.555D-3
5*12
6*900.15
5*0.2
HEAT17
1 5
0.8678D-6
4.465D-3 4.683D-3 4.901D-3 5.117D-3 5.337D-3 5.555D-3
5*12
6*900.15
5*0.2
HEAT18
1 5

```

0.8678D-6  
 4.465D-3 4.683D-3 4.901D-3 5.117D-3 5.337D-3 5.555D-3  
 5\*12  
 6\*900.15  
 5\*0.2  
 HEAT19  
 1 5  
 0.8678D-6  
 4.465D-3 4.683D-3 4.901D-3 5.117D-3 5.337D-3 5.555D-3  
 5\*12  
 6\*900.15  
 5\*0.2  
 HEAT20  
 1 5  
 0.8678D-6  
 4.465D-3 4.683D-3 4.901D-3 5.117D-3 5.337D-3 5.555D-3  
 5\*12  
 6\*900.15  
 5\*0.2  
 HEAT21  
 1 5  
 0.8678D-6  
 4.465D-3 4.683D-3 4.901D-3 5.117D-3 5.337D-3 5.555D-3  
 5\*12  
 6\*900.15  
 5\*0.2  
 HEAT22  
 1 5  
 0.8678D-6  
 4.465D-3 4.683D-3 4.901D-3 5.117D-3 5.337D-3 5.555D-3  
 5\*12  
 6\*900.15  
 5\*0.2  
 HEAT23  
 1 5  
 0.8678D-6  
 4.465D-3 4.683D-3 4.901D-3 5.117D-3 5.337D-3 5.555D-3  
 5\*12  
 6\*900.15  
 5\*0.2  
 HEAT24  
 1 5  
 0.8678D-6  
 4.465D-3 4.683D-3 4.901D-3 5.117D-3 5.337D-3 5.555D-3  
 5\*12  
 6\*900.15  
 5\*0.2  
 HEAT25  
 1 5  
 0.8678D-6  
 4.465D-3 4.683D-3 4.901D-3 5.117D-3 5.337D-3 5.555D-3  
 5\*12  
 6\*900.15  
 5\*0.2

```

HEAT26
  1 5
  0.8678D-6
  4.465D-3 4.683D-3 4.901D-3 5.117D-3 5.337D-3 5.555D-3
  5*12
  6*900.15
  5*0.2
HEAT27
  1 5
  0.8678D-6
  4.465D-3 4.683D-3 4.901D-3 5.117D-3 5.337D-3 5.555D-3
  5*12
  6*900.15
  5*0.2
HEAT28
  1 5
  0.8678D-6
  4.465D-3 4.683D-3 4.901D-3 5.117D-3 5.337D-3 5.555D-3
  5*12
  6*900.15
  5*0.2
HEAT29
  1 5
  0.8678D-6
  4.465D-3 4.683D-3 4.901D-3 5.117D-3 5.337D-3 5.555D-3
  5*12
  6*900.15
  5*0.2
HEAT30
  1 5
  0.8678D-6
  4.465D-3 4.683D-3 4.901D-3 5.117D-3 5.337D-3 5.555D-3
  5*12
  6*900.15
  5*0.2
HEAT01 1 -10 PIPE1 1 0 0 0
HEAT02 1 -10 PIPE1 2 0 0 0
HEAT03 1 -10 PIPE1 3 0 0 0
HEAT04 1 -10 PIPE1 4 0 0 0
HEAT05 1 -10 PIPE1 5 0 0 0
HEAT06 1 -10 PIPE1 6 0 0 0
HEAT07 1 -10 PIPE1 7 0 0 0
HEAT08 1 -10 PIPE1 8 0 0 0
HEAT09 1 -10 PIPE1 9 0 0 0
HEAT10 1 -10 PIPE1 10 0 0 0
HEAT11 2 -10 PIPE2 1 0 0 0
HEAT12 2 -10 PIPE2 2 0 0 0
HEAT13 2 -10 PIPE2 3 0 0 0
HEAT14 2 -10 PIPE2 4 0 0 0
HEAT15 2 -10 PIPE2 5 0 0 0
HEAT16 2 -10 PIPE2 6 0 0 0
HEAT17 2 -10 PIPE2 7 0 0 0
HEAT18 2 -10 PIPE2 8 0 0 0
HEAT19 2 -10 PIPE2 9 0 0 0

```



HEAT20	2	-10	PIPE2 10	0	0	0
HEAT21	2	-10	PIPE2 11	0	0	0
HEAT22	2	-10	PIPE2 12	0	0	0
HEAT23	2	-10	PIPE2 13	0	0	0
HEAT24	2	-10	PIPE2 14	0	0	0
HEAT25	2	-10	PIPE2 15	0	0	0
HEAT26	2	-10	PIPE2 16	0	0	0
HEAT27	2	-10	PIPE2 17	0	0	0
HEAT28	2	-10	PIPE2 18	0	0	0
HEAT29	2	-10	PIPE2 19	0	0	0
HEAT30	2	-10	PIPE2 20	0	0	0

## Appendix B Physical Properties of Freon-113

In order to analyse Aritomi's test of IAFB using Freon-113, physical properties of Freon-113 must be implemented into MINCS because they were not prepared in MINCS. The following physical properties of Freon-113 were used. They were from Prof. M.Aritomi of Tokyo Institute of Technology.

## 1. Unit of parameters

Pressure (p)	:	kg/cm <sup>2</sup>
Temperature (T)	:	°C
Enthalpy (h)	:	kcal/kg
Density ( $\rho$ )	:	kg/m <sup>3</sup>
Thermal conductivity(k)	:	kcal/(m.h.°C)
Viscosity ( $\mu$ )	:	kg.sec/m <sup>2</sup>
Specific heat (Cp)	:	kcal/(kg.°C)
Surface tension ( $\sigma$ )	:	kg/m

2. Saturation temperature  $T_s = F(p)$ 

$$T_s = -4.3123p^2 + 35.207p + 15.774 \quad (B-1)$$

3. Density of saturated vapour  $\rho_{vs} = F(T_s)$ 

$$\rho_{vs} = \frac{1}{0.44919 \times 10^{-4} T_s^2 - 0.82123 \times 10^{-2} T_s + 0.42434} \quad (B-2)$$

4. Density of liquid  $\rho_l = f(T_l)$ 

$$\rho_l = \frac{1}{0.35809 \times 10^{-6} T_l^2 + 0.74652 \times 10^{-6} T_l + 0.61844 \times 10^{-3}} \quad (B-3)$$

5. Enthalpy of saturated vapour  $h_{vs} = F(T_s)$ 

$$h_{vs} = -0.35672 \times 10^{-4} T_s^2 + 0.15126 T_s + 0.13819 \times 10^3 \quad (B-4)$$

6. Enthalpy of liquid  $h_l = F(T_l)$ 

$$h_l = 0.23987 \times 10^{-3} T_l^2 + 0.20296 T_l + 0.10004 \times 10^3 \quad (B-5)$$

7. Surface tension  $\sigma = F(T_s)$ 

$$\sigma = -0.10708 \times 10^{-4} T_s + 0.20395 \times 10^{-2} \quad (B-6)$$

8. Viscosity of vapour  $\mu_v = F(T_v)$   

$$\mu_v = -0.18330 \times 10^{-11} T_v^2 + 0.25884 \times 10^{-8} T_v + 0.98374 \times 10^{-6} \quad (B-7)$$

9. Viscosity of liquid  $\mu_l = F(T_l)$   

$$\mu_l = 0.68142 \times 10^{-8} T_l^2 - 0.12355 \times 10^{-5} T_l + 0.94316 \times 10^{-4} \quad (B-8)$$

10. Specific heat of vapour  $C_{p_v} = F(T_v)$   

$$C_{p_v} = 2.0 \times 0.34639 \times 10^{-4} T_v + 0.15846 \quad (B-9)$$

11. Specific heat of liquid  $C_{p_l} = F(T_l)$   

$$C_{p_l} = 2.0 \times 0.23987 \times 10^{-3} T_l + 0.20296 \quad (B-10)$$

12. Thermal conductivity of vapour  $k_v = F(T_v)$   

$$k_v = 0.32607 \times 10^{-7} T_v^2 + 0.35418 \times 10^{-4} T_v + 0.65874 \times 10^{-2} \quad (B-11)$$

13. Thermal conductivity of liquid  $k_l = F(T_l)$   

$$k_l = -0.20528 \times 10^{-7} T_l^2 - 0.19100 \times 10^{-3} T_l + 0.70589 \times 10^{-1} \quad (B-12)$$

14. To obtain superheated vapour temperature from  $T_s, h_v$  and  $h_{vs}$ ,  
 $T_v = F(T_s, h_v, h_{vs})$

$$T_v = \frac{-B + \sqrt{B^2 - 4 \times A \times C}}{2 \times A} \quad (B-13)$$

$$A = 0.34639 \times 10^{-4}$$

$$B = 0.15843$$

$$C = h_{vs} - h_v - B \times T_s - A \times T_s^2$$

15. To obtain liquid temperature from  $h_l$   $T_l = F(h_l)$

$$T_l = \frac{-B + \sqrt{B^2 - 4 \times A \times C}}{2 \times A} \quad (B-14)$$

$$A = 0.23987 \times 10^{-3}$$

$$B = 0.20296$$

$$C = 0.10004 \times 10^3 - h_l$$

Comparing them with experimental data from the Freon Company, it is found that their agreement is good in the pressure range of 0.5 to 3.0 kg/cm<sup>2</sup> as shown in Fig.B-1.

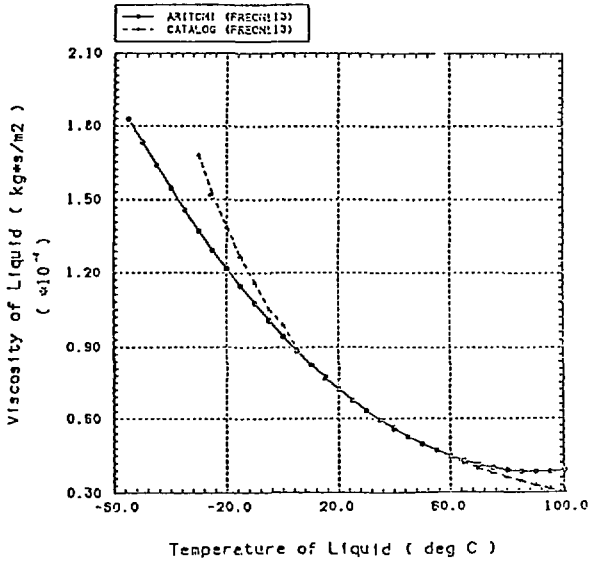


Fig. B-1a Comparison of viscosity of liquid.

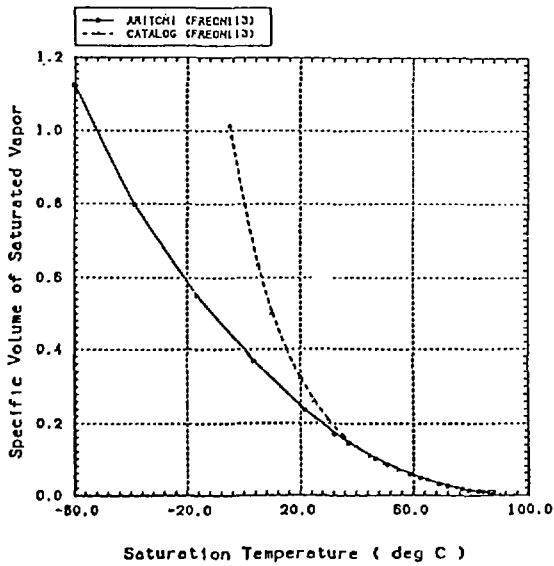


Fig. B-1b Comparison of specific volume.